e-ISSN 2320 –7876 www.ijfans.org
Vol.11, Iss.9, Dec 2022

Research Paper

Urea assisted microwave combustion synthesis and magnetic characterizations of spinel Co-$NiAl_2O_4$ nanoparticles

K. Mullai[1,*], G. Padma Priya[1]
[1] Department of Chemistry, Faculty of Arts and Science,
Bharath Institute of Higher Education and Research (BIHER),
Chennai – 600073, Tamil Nadu, India
***Corresponding Author Email addresses:** mulllaimadhu75@gmail.com (K. Mullai)

Address for Correspondence

K. Mullai[1,*], G. Padma Priya[1]
[1] Department of Chemistry, Faculty of Arts and Science,
Bharath Institute of Higher Education and Research (BIHER),
Chennai – 600073, Tamil Nadu, India
***Corresponding Author Email addresses:** mulllaimadhu75@gmail.com (K. Mullai)

Abstract

Spinel Co-$NiAl_2O_4$ nanoparticles were synthesized by a green combustion synthesis. Powder XRD patterns confirmed the formation of single phase spinel structure without other impurities. The average crystallite sizes (D) were estimated using Scherrer's method, and it was found to be in the range of 18.44 nm to 29.23 nm. FT-IR spectra showed vibrational stretching frequencies corresponding to the spinel structure. HR-SEM and TEM images showed the features of well particle shaped crystals with nano-sized grains. The elemental compositions of Co, Ni, Al and O were quantitatively obtained from EDX analysis. VSM measurements revealed that Co doped $NiAl_2O_4$ samples have superparamagnetism.

Keywords: Spinel Co-$NiAl_2O_4$; Urea; Nanoparticles; Magnetic properties.

1. Introduction

According to the distribution of cations in tetrahedral (A-) and octahedral (B-) sites, spinels are classified into normal and inverse structure. In normal spinel, the divalent (A^{2+}) cations on A-sites and the trivalent (B^{3+}) cations on B-sites, and is represented by the formula $^{IV}(A^{2+})^{VI}(B^{3+}B^{3+})O_4$. However, the inverse spinel, with the formula $^{IV}(B^{3+})^{VI}(A^{2+}B^{3+})O_4$, in which the divalent cations occupy the B-sites and the trivalent cations are equally divided among A- and B-sites, where, A and B represents the divalent (Co^{2+}, Ni^{2+}, Cu^{2+}, Zn^{2+}, etc.) and trivalent

(Fe^{3+}, Al^{3+}, etc.) cations occupying A- and B- sites, respectively, of a cubic crystal structure with a space group Fd-3m [1- 4]. Nanocrystalline spinels are a class of binary transition metal oxide semiconductors signify an attractive materials, which owing to their small size; exhibits novel physicochemical properties.

Among various binary transition metal oxides, $NiAl_2O_4$, has gained lot of interest in multidisciplinary areas, due to their effectiveness in ceramics, electronic, optical, catalyst, catalyst supports, aerospace, paints, dielectrics and sensing applications [2-5]. Spinel $NiAl_2O_4$ is a direct wide band gap semiconductor with optical band gap value of about 3.8 eV and may find applications in optoelectronic devices operated in the ultraviolet region. Spinel $NiAl_2O_4$ offers many beneficial properties such as high mechanical strength, high thermal stability, low surface acidity, and better diffusion, low temperature sintering ability, high chemical stability, wide band-gap energy, hydrophobic behavior, excellent optical transparency, good metal dispersion capacity, low surface acidity and high quantum yields [6, 7]. Also, $NiAl_2O_4$ is a semiconductor suitable for ultraviolet photoelectronic application [8].

Several methods have been used for the preparation of nanocrystalline $NiAl_2O_4$ such as hydroxide precursors, microwave assisted hydrothermal, co-precipitation, sol-ge, hydrothermal, combustion and solid-state reaction methods [9-16]. However, the above methods need sophisticated equipment and are expensive. The main disadvantages of the high temperature in sol-gel, co-precipitation and other methods are that the products obtained with higher particle size typically possess low surface area and inhomogeneity. Moreover, the above methods claims costly materials that generate toxic organic/inorganic intermediates and laborious synthetic procedures, thus leading to the tedious polluting process. Also, the above methods of preparation procedures were performed for long-time with high temperature.

However, the high surface area with a porous structure of $NiAl_2O_4$ is of great importance for catalytic activity. Therefore, in the present study, an attempt is given to synthesize single phase and porous $NiAl_2O_4$ with high specific surface area using urea as the fuel by the simple microwave combustion method (MCM). Recently, a novel method has been developed with the purpose of obtaining nanocrystalline solid materials with porous structure and high surface area, called microwave-assisted combustion method (MCM). In this method, the samples are prepared

at low temperatures, low cost with good control of size, structure and morphology. Mixed oxides obtained by MCM synthesis are usually nanocrystalline materials with well controlled size, morphology and chemical composition with very interesting textural properties [17-20].

2. Experimental part

2.1. Materials and methods

All the chemicals used in this study were of analytical grade obtained from Merck, India and were used as received without further purification. All chemicals such as nitrates of zinc, cobalt and aluminum, urea solution as the raw materials were used for this method. Millipore water was used for the entire preparation process of the samples.

In the preparation of $NiAl_2O_4$ sample, zinc nitrate (5 mmol) and aluminium nitrate (10 mmol) were first dissolved in urea solution under vigorous stirring at room temperature for 1 h until a clear transparent solution was obtained and were placed in a domestic microwave oven (SAMSUNG, India Limited) and exposed to the microwave energy in a 2.45 GHz multimode cavity at 850 W for 10 min. Initially, the precursor mixture boiled and underwent evaporation followed by the decomposition with the evolution of gases. When the solution attained the point of spontaneous combustion, ignition took place resulting in a rapid flame and yielding solid fluffy final products of mixed metal oxides. After completion of the reaction, the obtained solid powder was then washed with ethanol and dried at 70 ºC for 1h. The obtained powders were used for further characterization.

2.2. Characterization techniques

The structural characterization of spinel Co-$NiAl_2O_4$ NPs were performed using a Rigaku Ultima X-ray diffractometer (XRD) for 2θ values ranging from 10 to 80˚ using Cu-Kα radiation (λ = 1.5418 Å). Structural refinements using the Rietveld method was carried out using PDXL program; both refined lattice parameters and crystallite size of the obtained powders were reported. The surface functional groups were analyzed by Perkin Elmer FT-IR spectrometer. The surface morphology of the samples was achieved at desired magnification with a Joel JSM 6360 high resolution scanning electron microscope (HR-SEM) equipped with energy dispersive X-ray (EDX) for elemental composition analysis. The transmission electron micrographs were carried out by Philips-TEM (CM20). Magnetic measurements were carried out at room temperature

using a PMC MicroMag 3900 model vibrating sample magnetometer (VSM) equipped with 1 Tesla magnet.

3. Results and discussion

3.1. Structural analysis

Powder X-ray diffraction (XRD) analysis was used to investigate the phase structure and average crystallite size of the spinel Co-$NiAl_2O_4$ NPs. Fig. 1 shows the typical XRD patterns of spinel Co-$NiAl_2O_4$ NPs obtained at a different concentration of Co^{2+} dopant. The characteristic peaks at 2θ of 31.24, 36.77, 38.72, 44.79, 49.11, 55.78, 59.42, 65.37, 74.29 and 77.56° are corresponding to (220), (311), (222), (400), (331), (422), (511), (440), (620) and (533) diffraction planes. According to the XRD patterns, all diffraction peaks can be perfectly indexed as centered cubic spinel structured $NiAl_2O_4$ (JCPDS card no. 05-0665). The intensities and position of the peaks of the synthesized powders are in agreement with those of standard JCPDS and no other peak of any phase was detected, which indicates that the prepared samples were pure crystalline materials [21-25].

The average crystallite size calculated from the most intense X-ray diffraction peak (311) using scherrer's Eq. (1),

$$D = \frac{0.89\lambda}{\beta \cos\theta} \qquad \text{---- (1)}$$

where 'D' is the crystallite size, 'λ' , the X-ray wavelength, 'θ', the Bragg diffraction angle and 'β', the full width at half maximum (FWHM). The average crystallite size was estimated by applying the Scherrer's equation on the peak at 2θ = 36.75° for all samples. It was found that the average crystallite size 29.25 nm. The XRD broadening peaks in spinel Co-$NiAl_2O_4$ NPs strongly suggest that Co^{2+} ions were successfully substituted into $NiAl_2O_4$ host structure.

e-ISSN 2320 –7876 www.ijfans.org
Vol.11, Iss.9, Dec 2022

Research Paper

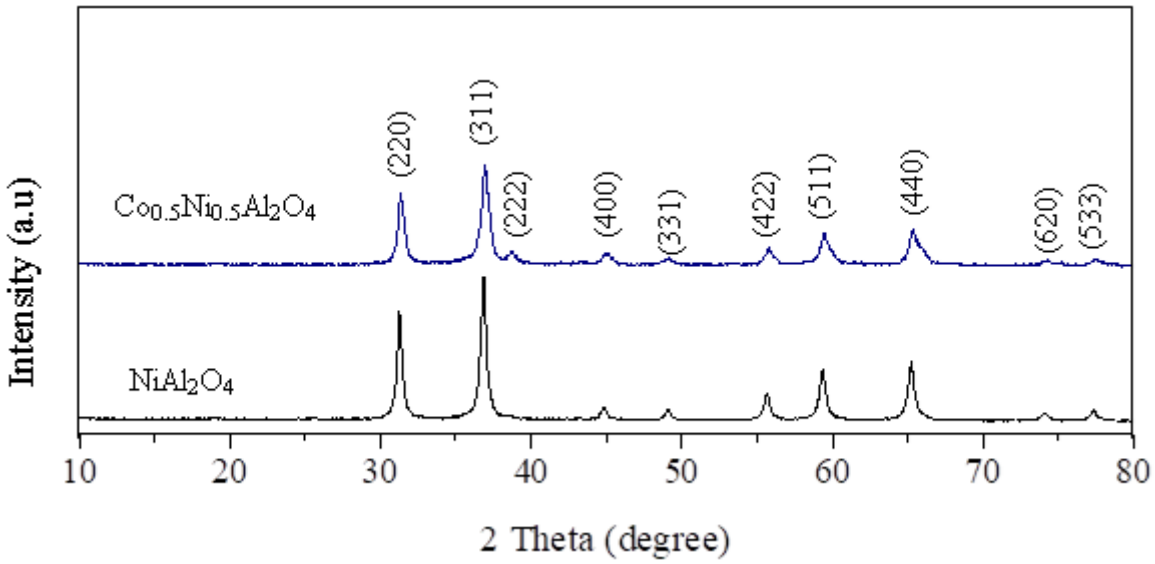

Fig. 1. Powder XRD patterns of Co-$NiAl_2O_4$ NPs.

3.2 FT-IR analysis

FT-IR spectra of spinel Co-$NiAl_2O_4$ NPs are shown in Fig. 2. Free water molecule has a strong and broad absorption band centered in the region 3120-3400 cm^{-1}. It can be seen that the bands at around 3432 cm^{-1} and at around 1635 cm^{-1} are present in all compositions, which can be assigned to the -OH stretching and H-O-H bending vibrations of adsorbed H_2O, respectively. The absorption band at 2342 cm^{-1} is due to the stretching vibration of CO_2 from atmosphere. In all compositions of $NiAl_2O_4$ samples, the metal-oxygen stretching frequencies are reported in the range 500-900 cm^{-1}, associated with the vibrations of M-O, Al-O and M-O-Al bonds (M = Ni, Co) [26-30]. Generally, FT-IR spectra was measured in air atmosphere condition, which results in rapid adsorption of H_2O from the atmosphere, due to the very high surface area of the as-prepared spinel nano-crystals [31-35].

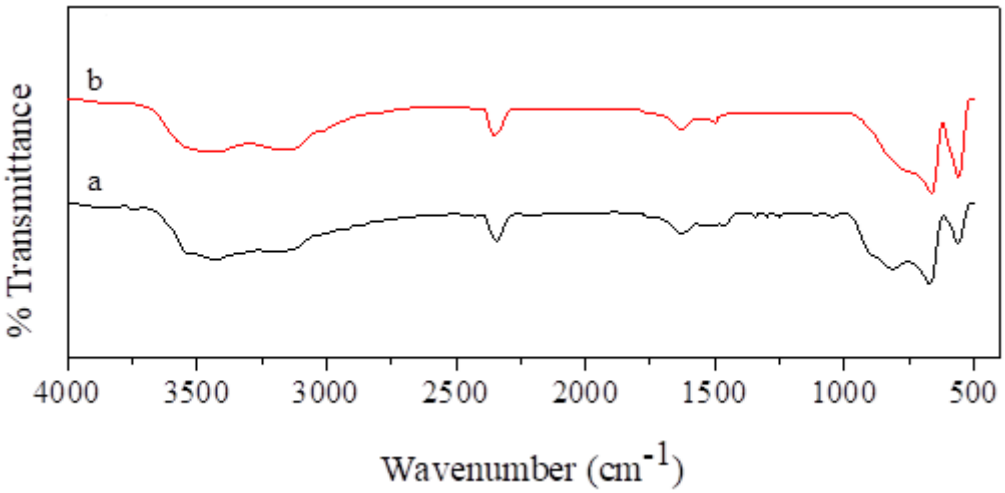

Fig. 2. FT-IR spectrum of Co-$NiAl_2O_4$ NPs.

3.3 SEM studies

Fig. 3 shows HR-SEM images of spinel Co-$NiAl_2O_4$ NPs. However, the surface morphologies of spinel Co-$NiAl_2O_4$ NPs as seen from the HR-SEM consists of well developed particles with different shape and size of crystals with less uniform; varying size distribution with relatively well crystallized grain size smaller than 50 nm [36-38].

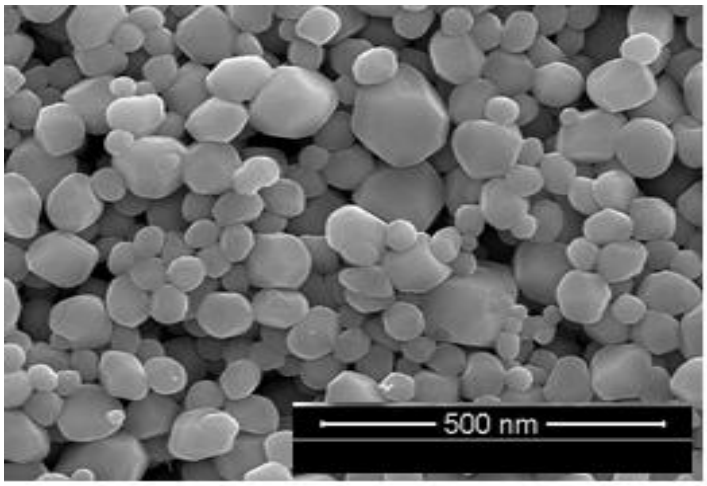

Fig. 3. SEM image of Co-$NiAl_2O_4$ NPs.

3.4. TEM studies

The average crystallite size estimated from the XRD and Rietveld refinement XRD data agree with HR-TEM investigations. HR-TEM images of spinel Co-$NiAl_2O_4$ NPs are provided in

Fig. 4. The small amount of agglomerations was observed in the HR-TEM micrographs. However, these nanoparticles are in the range of 20-30 nm in diameter; these values are in good agreement with the values obtained from XRD data [39-42]. The selected area electron diffraction (SAED) patterns, presented in the Fig. 4, correspond to that of a spinel phase, confirm that the nano-crystals are composed of $NiAl_2O_4$.

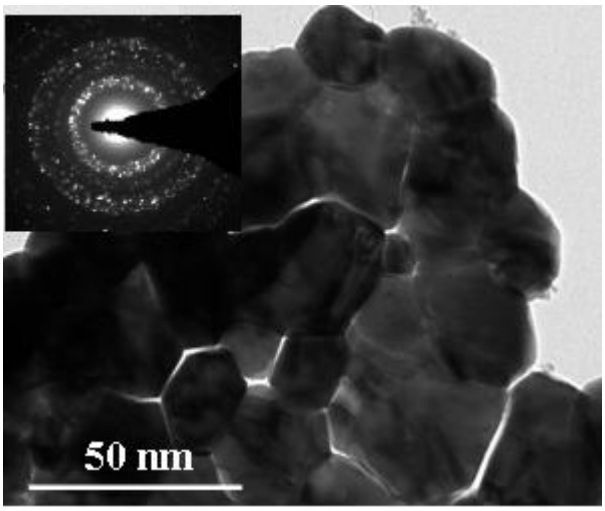

Fig. 4. TEM image of Co-$NiAl_2O_4$ NPs.

3.5 EDX studies

Energy dispersive X-ray (EDX) analysis of the as-prepared spinel Co-$NiAl_2O_4$ NPs is shown in Fig. 5. EDX results showed that the peaks of Ni, Al and O elements and there is no other peak, which confirmed the as-prepared samples are pure. A small peak is appeared at 2.1 KeV for all the samples, which indicated the presence of gold (Au), which has been used as a sputter coating, while preparing the sample for HR-SEM analysis for the better visibility of the surface morphology.

e-ISSN 2320 –7876 www.ijfans.org
Vol.11, Iss.9, Dec 2022

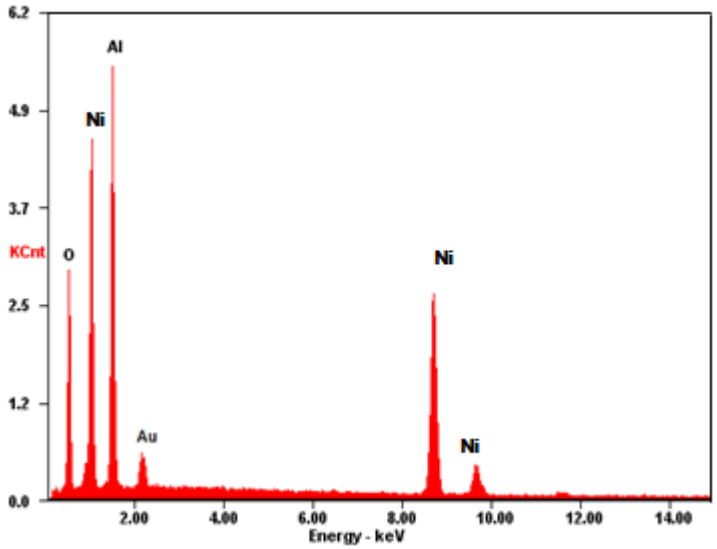

Fig. 5. EDX spectra of Co-$NiAl_2O_4$ NPs.

3.6 Magnetic measurements

The magnetization behavior of spinel Co-$NiAl_2O_4$ NPs were investigated by sweeping the external magnetic field between ±15 kOe at 300 K using room temperature vibrating sample magnetometer (VSM). These curves are typical for a soft magnetic material and indicate hysteresis dia, superpara and ferromagnetism in the field ranges of ±15 kOe. A small hysteresis was observed for $NiAl_2O_4$ sample shows of superparamagnetism behavior [43-46].

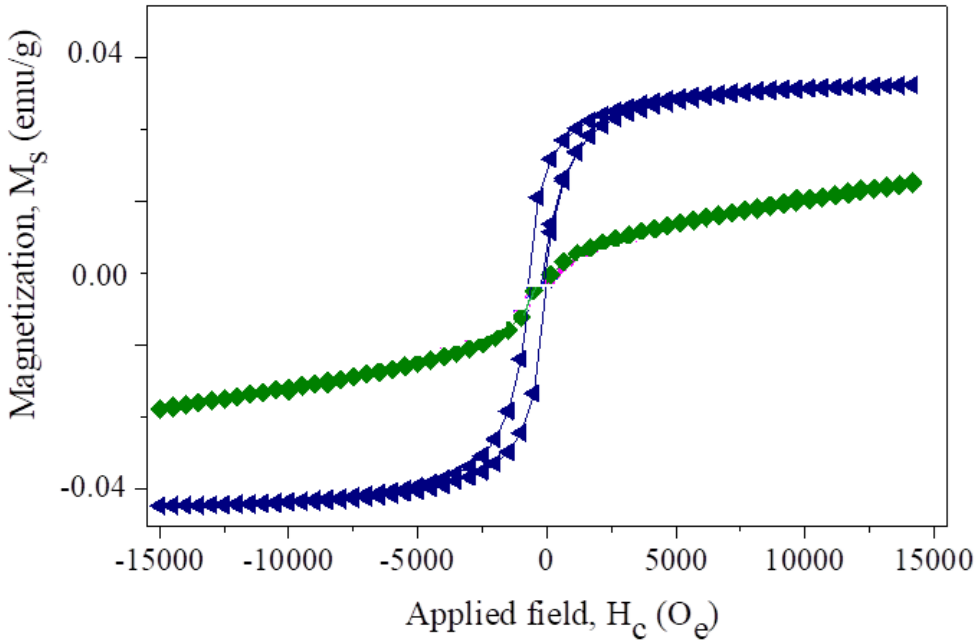

Fig. 6. VSM measurements of Co-$NiAl_2O_4$ NPs.

4. Conclusions

Spinel Co-$NiAl_2O_4$ NPs were successfully prepared by a simple MCM route using metal nitrates and urea as raw materials. Powder XRD pattern suggested the formation of pure gahnite in all the Co^{2+} doped $NiAl_2O_4$ matrices. Also, the XRD, EDX and SAED results indicate that the as-synthesized spinel Co-$NiAl_2O_4$ NPs have spinel structure without the presence of any other phase impurities. The appearance of two bands between 500 and 900 cm^{-1} in FT-IR spectra revealed the formation of spinel structure. HR-SEM and HR-TEM images depicted the formation of well developed particle-like crystal morphology with nano-sized grains. VSM study revealed that the doping of Co^{2+} in $NiAl_2O_4$ can bring in superparamagnetic behavior.

References

1. K. Chinnaraj, A. Manikandan, P. Ramu, S. Arul Antony, P. Neeraja, Comparative study of microwave and sol-gel assisted combustion methods of Fe_3O_4 nanostructures: Structural, morphological, optical, magnetic and catalytic properties, Journal of Superconductivity and Novel Magnetism, 28 (2015) 179-190.
2. E. Hema, A. Manikandan, P.Karthika, M. Durka, S. Arul Antony, B. R. Venkatraman, A novel synthesis of Zn^{2+}-doped $CoFe_2O_4$ spinel nanoparticles: Structural, morphological, opto-magnetic and catalytic properties, Journal of Superconductivity and Novel Magnetism, 28 (2015) 2539-2552.
3. V. Umapathy, A. Manikandan, S. Arul Antony, P. Ramu, P. Neeraja, Synthesis, structural, morphological and opto-magnetic properties of Bi_2MoO_6 nano-photocatalyst by sol-gel method, Transactions of Nonferrous Metals Society of China, 25 (2015) 3271-3278.
4. A. Manikandan, S. Arul Antony, R. Sridhar, Seeram Ramakrishna, M. Bououdina, A simple combustion synthesis and optical studies of magnetic $Zn_{1-x}Ni_xFe_2O_4$ nanostructures for photoelectrochemical applications, Journal of Nanoscience and Nanotechnology, 15 (2015) 4948-4960.

5. A. Manikandan, M. Durka, S. Arul Antony, Magnetically recyclable spinel $Mn_xZn_{1-x}Fe_2O_4$; ($0.0 \leq x \leq 0.5$) nano-photocatalysts, Advanced Science, Engineering and Medicine, 7 (2015) 33-46.
6. A. Manikandan, A. Saravanan, S. Arul Antony, M. Bououdina, One-pot low temperature synthesis and characterization studies of nanocrystalline α-Fe_2O_3 based dye sensitized solar cells, Journal of Nanoscience and Nanotechnology, 15 (2015) 4358-4366.
7. M. F. Valan, A. Manikandan, S. Arul Antony, A novel synthesis and characterization studies of magnetic Co_3O_4 nanoparticles, Journal of Nanoscience and Nanotechnology, 15 (2015) 4580-4586.
8. M. F. Valan, A. Manikandan, S. Arul Antony, Microwave combustion synthesis and characterization studies of magnetic $Zn_{1-x}Cd_xFe_2O_4$ ($0 \leq x \leq 0.5$) nanoparticles, Journal of Nanoscience and Nanotechnology, 15 (2015) 4543-4551.
9. K. Chitra, K. Reena, A. Manikandan, S. Arul Antony, Antibacterial studies and effect of poloxamer on gold nanoparticles by Zingiber officinale extracted green synthesis, Journal of Nanoscience and Nanotechnology, 15 (2015) 4984-4991.
10. S. Jayasree, A. Manikandan, A. M. Uduman Mohideen, C. Barathiraja, S. Arul Antony, Comparative study of combustion methods, opto-magnetic and catalytic properties of spinel $CoAl_2O_4$ nano- and microstructures, Advanced Science, Engineering and Medicine, 7 (2015) 672-682.
11. D. K. Manimegalai, A. Manikandan, S. Moortheswaran, S. Arul Antony, One-pot microwave irradiation synthesis and characterization studies of nanostructured CdS photo-catalysts, Advanced Science, Engineering and Medicine, 7 (2015) 722-727.
12. A. Mary Jacintha, A. Manikandan, K. Chinnaraj, S. Arul Antony, P. Neeraja, Comparative studies of spinel $MnFe_2O_4$ nanostructures: Structural, morphological, optical, magnetic and catalytic properties, Journal of Nanoscience and Nanotechnology, 15 (2015) 9732-9740.
13. G. Padmapriya, A. Manikandan, V. Krishnasamy, S. K. Jaganathan, S. Arul Antony, Spinel $Ni_xZn_{1-x}Fe_2O_4$ ($0.0 \leq x \leq 1.0$) nano-photocatalysts: Synthesis, characterization and photocatalytic degradation of methylene blue dye, Journal of Molecular Structure, 1119 (2016) 39-47.

14. A. Manikandan, M. Durka, S. Arul Antony, Hibiscus rosa-sinensis leaf extracted green methods, magneto-optical and catalytic properties of spinel $CuFe_2O_4$ nano- and microstructures, Journal of Inorganic and Organometallic Polymers and Materials, 25 (2015) 1019–1031.
15. A. Manikandan, M. Durka, K. Seevakan, S. Arul Antony, A novel one-pot combustion synthesis and opto-magnetic properties of magnetically separable spinel $Mn_xMg_{1-x}Fe_2O_4$ ($0.0 \leq x \leq 0.5$) nano-photocatalysts, Journal of Superconductivity and Novel Magnetism, 28 (2015) 1405-1416.
16. A. Manikandan, M. Durka, S. Arul Antony, One-pot flash combustion synthesis, structural, morphological and opto-magnetic properties of spinel $Mn_xCo_{1-x}Al_2O_4$ (x = 0, 0.3 and 0.5) nano-catalysts, Journal of Superconductivity and Novel Magnetism, 28 (2015) 209–218.
17. A. Manikandan, E. Hema, M. Durka, M. Amutha Selvi, T. Alagesan, S. Arul Antony, Mn^{2+} doped NiS ($Mn_xNi_{1-x}S$: x = 0.0, 0.3 and 0.5) nanocrystals: Structural, morphological, opto-magnetic and photocatalytic properties, Journal of Inorganic and Organometallic Polymers and Materials, 25 (2015) 804–815.
18. A. Manikandan, E. Hema, M. Durka, K. Seevakan, T. Alagesan, S. Arul Antony, Room temperature ferromagnetism of magnetically recyclable photocatalyst of $Cu_{1-x}Mn_xFe_2O_4$-TiO_2 ($0.0 \leq x \leq 0.5$) nano-composites, Journal of Superconductivity and Novel Magnetism, 28 (2015) 1783-1795.
19. A. Manikandan, M. Durka, S. Arul Antony, Role of Mn^{2+} doping on structural, morphological and opto-magnetic properties of spinel $Mn_xCo_{1-x}Fe_2O_4$ (x = 0.0, 0.1, 0.2, 0.3, 0.4 and 0.5) nano-catalysts, Journal of Superconductivity and Novel Magnetism, 28 (2015) 2047–2058.
20. G. Mathubala, A. Manikandan, S. Arul Antony and P. Ramar, Photocatalytic degradation of methylene blue dye and magneto-optical studies of magnetically recyclable spinel $Ni_xMn_{1-x}Fe_2O_4$ (x = 0.0-1.0) nanoparticles, J. of Molecular Structure, 1113 (2016) 79-87.
21. V. Mary Teresita, A. Manikandan, B. Avila Josephine, S. Sujatha, S. Arul Antony, Electro-magnetic properties and humidity sensing studies of magnetically recoverable $LaMg_xFe_{1-}$

$_xO_{3-\delta}$ perovskites nano-photocatalysts by sol-gel route, Journal of Superconductivity and Novel Magnetism, 29 (2016) 1691–1701.

22. S. Jayasree, A. Manikandan, S. Arul Antony, A. M. Uduman Mohideen, C. Barathiraja, Magneto-optical and catalytic properties of recyclable spinel $NiAl_2O_4$ nanostructures using facile combustion methods, Journal of Superconductivity and Novel Magnetism, 29 (2016) 253–263.
23. C. Barathiraja, A. Manikandan, A. M. Uduman Mohideen, S. Jayasree, S. Arul Antony, Magnetically recyclable spinel $Mn_xNi_{1-x}Fe_2O_4$ (x = 0.0–0.5) nano-photocatalysts: Structural, morphological and opto-magnetic properties, Journal of Superconductivity and Novel Magnetism, 29 (2016) 477-486.
24. B. Avila Josephine, A. Manikandan, V. Mary Teresita, S. Arul Antony, Fundamental study of $LaMg_xCr_{1-x}O_{3-\delta}$ perovskites nano-photocatalysts: Sol-gel synthesis, characterization and humidity sensing, The Korean Journal of Chemical Engineering, 33 (2016) 1590-1598.
25. A. Manikandan, M. Durka, M. A. Selvi, S. Arul Antony, Sesamum indicum plant extracted microwave combustion synthesis and opto-magnetic properties of spinel $Mn_xCo_{1-x}Al_2O_4$ nano-catalysts, Journal of Nanoscience and Nanotechnology, 16 (2016) 448-456.
26. A. Manikandan, M. Durka, M. A. Selvi, S. Arul Antony, Aloe vera plant extracted green synthesis, structural and opto-magnetic characterizations of spinel $Co_xZn_{1-x}Al_2O_4$ nano-catalysts, Journal of Nanoscience and Nanotechnology, 16 (2016) 357-373.
27. A. Manikandan, S. Arul Antony, Magnetically separable $Mn_xZn_{1-x}Fe_2O_4$; ($0.0 \leq x \leq 0.5$) nanostructures: Structural, morphological, opto-magnetic and photocatalytic properties, Synthesis and Reactivity in Inorganic, Metal-Organic, and Nano-Metal Chemistry, 46 (2016) 1277-1297.
28. S. Rajmohan, A. Manikandan, V. Jeseentharani, S. Arul Antony, J. Pragasam, Simple co-precipitation synthesis and characterization studies of $La_{1-x}Ni_xVO_3$ perovskites nanostructures for humidity sensing applications, Journal of Nanoscience and Nanotechnology, 16 (2016) 1650-1655.
29. E. Hema, A. Manikandan, M. Gayathri, M. Durka, S. Arul Antony, B. R. Venkatraman, Role of Mn^{2+}-doping on structural, morphological, optical, magnetic and catalytic

properties of spinel $ZnFe_2O_4$ nanoparticles, Journal of Nanoscience and Nanotechnology, 16 (2016) 5929-5943.

30. E. Hema, A. Manikandan, P. Karthika, M. Durka, S. Arul Antony, B. R. Venkatraman, Magneto-optical properties of recyclable spinel $Ni_xMg_{1-x}Fe_2O_4$ ($0.0 \leq x \leq 1.0$) nano-catalysts, J. Nanoscience and Nanotechnology, 16 (2016) 7325-7336.
31. S. Moortheswaran, A. Manikandan, S. Sujatha, S. K. Jaganathan, S. Arul Antony, One-pot combustion synthesis and characterization studies of spinel $CoAl_2O_4$ nano-catalysts, Nanoscience and Nanotechnology Letters, 8 (2016) 424-427.
32. S. Moortheswaran, A. Manikandan, S. Sujatha, S. K. Jaganathan, S. Arul Antony, Selective catalytic oxidation of benzyl alcohol and characterization studies of spinel $MnAl_2O_4$ nanoparticles by a facile synthesis route, Nanoscience and Nanotechnology Letters, 8 (2016) 434-437.
33. P. Thilagavathi, A. Manikandan, S. Sujatha, S. K. Jaganathan, S. Arul Antony, Sol-gel synthesis and characterization studies of $NiMoO_4$ nanostructures for photocatalytic degradation of methylene blue dye, Nanoscience and Nanotechnology Letters, 8 (2016) 438-443.
34. S. Rajmohan, V. Jeseentharani, A. Manikandan, J. Pragasam, Co-precipitation synthesis method, characterizations and humidity sensing applications of perovskite-type mixed oxide $La_{1-x}Co_xVO_{3-\delta}$ nanocomposites, Nanoscience and Nanotechnology Letters, 8 (2016) 393-398.
35. K. Seevakan, A. Manikandan, P. Devendran, S. Arul Antony, T. Alagesan, One-pot synthesis and characterization studies of iron molybdenum mixed metal oxide ($Fe_2(MoO_4)_3$) nano-photocatalysts, Advanced Science, Engineering and Medicine, 8 (2016) 566-572.
36. G. Padmapriya, A. Manikandan, V. Krishnasamy, S. K. Jaganathan, S. Arul Antony, Enhanced catalytic activity and magnetic properties of spinel $Mn_xZn_{1-x}Fe_2O_4$ ($0.0 \leq x \leq 1.0$) nano-photocatalysts by microwave irradiation route, Journal of Superconductivity and Novel Magnetism, 29 (2016) 2141-2149.

37. S. Suguna, S. Shankar, S. K. Jaganathan, A. Manikandan, Novel synthesis of spinel $Mn_xCo_{1-x}Al_2O_4$ (x = 0.0 to 1.0) nano-catalysts: Effect of Mn^{2+} doping on structural, morphological and opto-magnetic properties, Journal of Superconductivity and Novel Magnetism, 30 (2017) 691–699.
38. S. Gunasekaran, K. Thanrasu, A. Manikandan, M. Durka, A. Dinesh, S. Anand, S. Shankar, Y.Slimani, M. A. Almessiere, A. Baykal, Structural, fabrication and enhanced electromagnetic wave absorption properties of reduced graphene oxide (rGO)/zirconium substituted cobalt ferrite ($Co_{0·5}Zr_{0·5}Fe_2O_4$) nanocomposites, Physica B: Condensed Matter, 605 (2021) 412784.
39. F. Hussain, S. Z. Shah, H. Ahmad, S. A. Abubshait, H. A. Abubshait, A. Laref, A. Manikandan, H. S. Kusuma, M. Iqbal, Microalgae an ecofriendly and sustainable wastewater treatment option: Biomass application in biofuel and bio-fertilizer production. A review, Renewable and Sustainable Energy Reviews, 137 (2021) 110603.
40. P. A. Vinosha, A. Manikandan, A. S. J. Ceicilia, A. Dinesh, G. F. Nirmala, A. Christy Preetha, Y. Slimani, M.A. Almessiere, A. Baykal, B. Xavier, Review on recent advances of zinc substituted cobalt ferrite nanoparticles: Synthesis characterization and diverse applications, Ceramics International, 47 (2021) 10512-10535.
41. Y. Slimani, N. A. Algarou, M. A. Almessiere, A. Sadaqat M. G. Vakhitov, D. S. Klygach, D. I. Tishkevich, A. V. Trukhanov, S. Güner, A. S. Hakeem, I. A. Auwal, A. Baykal, A. Manikandan, I. Ercan, Fabrication of exchanged coupled hard/soft magnetic nanocomposites: Correlation between composition, magnetic, optical and microwave properties, Arabian Journal of Chemistry, 10 (2021) 102992.
42. M. George, T.L. Ajeesha, A. Manikandan, Ashwini Anantharaman, R.S. Jansi, E. Ranjith Kumar, Y. Slimani, M.A. Almessiere, A. Baykal, Evaluation of Cu-$MgFe_2O_4$ spinel nanoparticles for photocatalytic and antimicrobial activates, Journal of Physics and Chemistry of Solids, 153 (2021) 110010.
43. S. S. Al-Jameel, M. A. Almessiere, F. A. Khan, N. Taskhandi , Y. Slimani, N. S. Al-Saleh, A. Manikandan, E. A. Al-Suhaimi, A. Baykal, Synthesis, Characterization, Anti-Cancer

Analysis of $Sr_{0.5}Ba_{0.5}Dy_xSm_xFe_{8-2x}O_{19}$ ($0.00 \leq x \leq 1.0$) Microsphere Nanocomposites, Nanomaterials, 11 (2021) 700.

44. M. A. Almessiere, Y. Slimani, H. Güngüneş, K. A. Demir, Z. Tatiana, T. Sergei, T. Alex, A. Manikandan, A. Fatimah, A. Baykal, Influence of Dy^{3+} ions on microstructure, magnetic, electrical and microwave properties of $[Ni_{0.4}Cu_{0.2}Zn_{0.4}](Fe_{2-x}Dy_x)O_4$ ($0.00<x<0.04$) spinel ferrites, ACS Omega, 6 (2021) 10266-10280.
45. P. Annie Vinosha, A. Manikandan, A. Christy Preetha, A. Dinesh, Y. Slimani, M.A. Almessiere, A. Baykal, Belina Xavier, G. Francisco Nirmala, Review on recent advances of synthesis, magnetic properties and water treatment applications of cobalt ferrite nanoparticles and nanocomposites, Journal of Superconductivity and Novel Magnetism, 34 (2021) 995–1018.
46. O. Alagha, N. Ouerfelli, H. Kochkar, M. A. Almessiere , Y. Slimani, A. Manikandan, A. Baykal, A. Mostafa, M. Zubair, M. H. Barghouthi, Kinetic Modeling for Photo-Assisted Penicillin G Degradation of $(Mn_{0.5}Zn_{0.5})[Cd_xFe_{2-x}]O_4$ ($x \leq 0.05$) Nanospinel Ferrites, Nanomaterials, 11 (2021) 970.